

Simulation of cluster ejection following high-energy $\text{Au}_n \rightarrow \text{Au}(111)$ bombardment

M.H. Shapiro^{a, b, *}, T.A. Tombrello^b

^a Department of Physics, California State University, P.O. Box 6866, Fullerton, CA 92834-6866, USA

^b Division of Physics, Mathematics and Astronomy, California Institute of Technology, Pasadena, CA 91125, USA

Received 27 September 1999; accepted for publication 25 January 2000

Abstract

Following the recent report by Andersen et al. of extremely large nonlinear sputtering yields caused by the bombardment of gold targets with small, high energy gold clusters [Phys. Rev. Lett. 80 (1998) 5433], we carried out simulations showing: (1) that the thermal spike phase of the collision cascade contributes significantly to these nonlinear yields; and (2) that individual ‘mega-events’ with yields up to ~ 2500 contribute significantly to the total sputtering yields [Shapiro and Tombrello, Nucl. Instrum. Meth. B 152 (1999) 221]. Here we extend our simulations to examine the cluster component of the sputtering yield. We find that clusters with $n \geq 2$ constitute a large fraction of the yield. In the early stages of sputtering (≤ 3 ps) clusters with as many as ~ 800 atoms are ejected. These very large clusters are not stable; however, after allowing the simulations to evolve for an additional 100 ps, clusters with as many as ~ 300 atoms remain. The yields of clusters with $n \leq \sim 10$ follow typical power law distributions, while the yield of clusters with $n > \sim 10$ significantly exceed the predictions of the power-law distribution. Our simulations also show that clusters with more than a few tens of atoms are emitted exclusively during the thermal spike phase. © 2000 Elsevier Science B.V. All rights reserved.

Keywords: Atomistic dynamics; Computer simulations; Gold; Ion–solid interactions; Molecular dynamics; Sputtering

1. Introduction

Andersen et al. [1] reported yield measurements for $\text{Au}_n \rightarrow \text{Au}$ sputtering with $1 \leq n \leq 5$ at bombarding energies ranging from ~ 20 keV atom⁻¹ to ~ 2 MeV atom⁻¹ for $n \leq 3$, and at bombarding energies ranging from ~ 20 to ~ 500 keV atom⁻¹ for $n = 4$ and $n = 5$. Very large nonlinearities were observed in these sputtering yields. For example, at 150 keV atom⁻¹ bombarding energy the yield

(Y) was ~ 3000 for Au_5 clusters, but only ~ 55 for monomers with the same energy. In an attempt to understand the origin of these large nonlinearities, we carried out molecular dynamics (MD) simulations on a massively parallel computer [2]. These simulations showed:

1. that the thermal spike phase of the collision cascade contributed significantly to the nonlinear yield, and
2. that individual sputtering events with very large yields (up to ~ 2500 atoms) contributed significantly to the total sputtering yield.

The emission of clusters is known to be correlated with individual events with large sputtering yields

* Corresponding author. Fax: +1-714-278-5810.

E-mail address: mshapiro@fullerton.edu (M.H. Shapiro)

[3]. However, the simulation program that was used in Ref. [2] did not include a search for clusters in the sputtered material.

In this study we repeated the simulations for the case of $100 \text{ keV atom}^{-1} \text{ Au}_n$ ions ($1 \leq n \leq 3$) incident on Au(111) targets, using programs that permitted us to search for ejected clusters both at the end of the sputtering simulations ($t = 3 \text{ ps}$) and after the sputtered material had evolved for an additional 100 ps. Our results show that:

1. a large fraction of the sputtered material is in the form of clusters at this bombarding energy;
2. very large clusters can be emitted in individual high-yield events;
3. clusters with more than a few tens of atoms are emitted exclusively during the thermal spike phase of the collision cascade; and
4. the number of large clusters present in the ejected material significantly exceeds the predictions of the power-law distribution.

2. Simulation model

The simulations reported in this paper were carried out on fast single processor workstations rather than the parallel computer used for the work reported in Ref. [2]. However, the part of the code that was used to compute trajectories was identical to that used previously with one minor exception. Following the termination of the simulation for each individual impact, the positions as well as the velocity components of each ejected atom were saved to a file, which allowed for a subsequent search for sputtered clusters.

In the previous simulations [2] we found that many impacts produced no sputtered atoms. Since the focus of this work was cluster ejection and the starting locations for each impact simulated in Ref. [2] were available, to save computer time only those impacts that had yields of 2 or more sputtered atoms were computed again using identical initial conditions. In addition, in this work only the impacts of $100 \text{ keV atom}^{-1} \text{ Au}_1$, Au_2 , and Au_3 ions with Au(111) targets were simulated.

The SPUT2 MD code used for these simulations

incorporates several features that enhance computational efficiency. These include a self-adjusting time step [4], neighbor-list logic [5], and a ‘moving atom’ list [5]. For these calculations with large targets (> 12000 atoms), the neighbor-list algorithm was modified to increase the speed of the code. In this modified version of the algorithm, atoms are placed on the neighbor-list only if they are:

1. moving; or
2. within the force cutoff distance of a moving atom; or
3. within the force cutoff range of atoms placed on the list because they satisfied criterion (2).

With this modification the size of the neighbor list grows only in proportion to the size of the developing collision cascade, which saves considerable computer time during the early stages of the collision cascade.

Electronic energy losses for valence electrons were accounted for with a viscous drag model, that is, $dE/dx = -Kv = -NS_e$, where N is the average electron density and S_e is the electronic stopping power [6]. A correction also was included to account for straggling [7]; however, this was an order of magnitude smaller than the viscous drag correction.

The fcc(111) targets used in these simulations had lateral dimensions of approximately $9.8 \text{ nm} \times 9.8 \text{ nm}$, and were nine layers thick. They contained a total of 12363 atoms. These dimensions were large enough to contain the lateral spread of most collision cascades, but the yields obtained for monomer impacts with the open boundary conditions used in the simulations typically were one-third to one-half of the yields observed experimentally. This can be attributed to a large fraction of the momentum in the collision cascades being transported through the back surface of the simulation targets. In thick targets some of this ‘lost’ momentum would be reflected back towards the target surface by collisions deeper in the target. Although atoms moving towards the surface from deep within a thick target seldom sputter, the momentum carried towards the surface increases the yield of atoms sputtered from the first several atomic layers.

To compensate for this effect a reflection algorithm was used. A fraction (10%) of the incident ions and target atoms reaching the back surface of the target had their velocity component along the beam direction reversed to simulate momentum coming back into the surface region from deeper in the target. To quench the effect only a single bounce from the back surface was permitted for any projectile. If any reflected atom reached the back surface a second time, it was permitted to continue out of the target. With a 10% reflection coefficient the total sputtering yield with the algorithm in operation was close to the experimentally observed yield for 100 keV Au₁ ions.

An ejected atom was considered to be sputtered if it had a velocity component along the beam direction that was negative (i.e. away from the target), and if it had moved away from the front surface of the target by at least twice the lattice constant (8.16 Å) before the integration was cutoff at 3 ps. This ensured that atoms were considered to be sputtered only if they were well beyond the range of forces from target atoms. The code that was used to search for clusters examined only those atoms that satisfied these criteria for sputtering. This procedure may have under-counted a few clusters, but it avoided counting clusters that might eventually return to the target surface.

The simulations reported here employed the same two-body Au–Au potential that was used in Ref. [2]. This potential includes a repulsive Molière core that is connected to an attractive Morse well with a cubic spline. The parameters for this potential have been published previously [8]. The parameters of the Morse potential have been adjusted to fit the bulk properties of gold. Typically, such potentials are too shallow to bind a free gold dimer properly [9], but would be expected to approach the experimentally observed binding for larger clusters. In comparison, the empirical many-body potentials that often are used in low-energy sputtering simulations tend to bind small clusters too tightly [3]. As a result the fraction of atoms that are bound in clusters can be overestimated significantly when such potentials are used. For example, in the study by Colla et al. [3] the Cu dimer fraction was overestimated by at

least a factor of 4 in MD simulations with two different many-body potentials.

In our previous studies of dimer ejection from Cu targets [10], we found little difference between the frequency of various dimer sputtering mechanisms computed with a two-body Morse potential and those dimer sputtering mechanisms computed with a many-body embedded atom potential that closely fit the free dimer binding energy – even though the absolute yields of dimers differed by about a factor of 3. A similar sensitivity to the choice of potentials can be expected for Au, which also is a closely packed fcc structure. While our use of two-body potentials was dictated primarily by the need to conserve computer time, the results obtained with them should not be considered inherently less reliable than those obtained with many-body potentials. Rather, as with all simulations, our results must be regarded as only an approximation to reality.

Once the trajectories for a given case had been recomputed, the output files were scanned for clusters using a program written specifically for that purpose. This program first identified bound dimer pairs. Then it identified larger clusters by searching for bonds between dimers. An atom was considered to belong to a cluster if it had a stable dimer bond to at least one other atom in the cluster. If an atom had more than one stable dimer bond to other atoms in the cluster, it was counted only once to make sure that the size of the cluster was not overstated.

Even though assemblies of atoms formed in this manner will have a total internal energy that is negative, they are not unconditionally stable. It is well known that the ‘hot’ clusters ejected in sputtering simulations can lose atoms through unimolecular decomposition [11] caused by the transfer of sufficient internal energy to an atom within the cluster to break its bond(s) with the remaining atoms in the cluster. It also is conceivable that large clusters could undergo more complicated decomposition modes. To account for these decomposition processes, the sputtered material (including all sputtered atoms and clusters) was ‘evolved’ for an additional 100 ps. This was done with an MD program that used the position and velocity components of the sputtered atoms as its

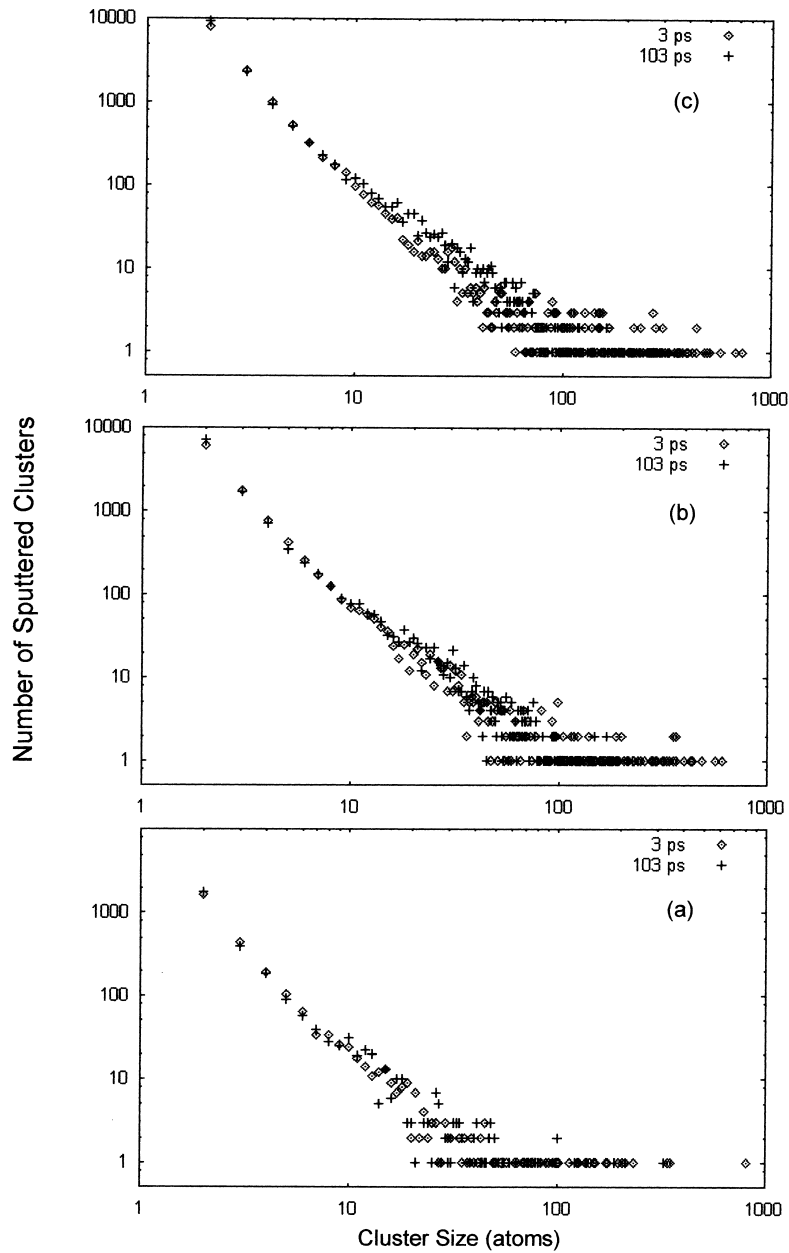


Fig. 1. Size distributions of emitted clusters following bombardment of Au(111) targets with (a) 100 keV Au₁ ions, (b) 100 keV atom⁻¹ Au₂ ions, and (c) 100 keV atom⁻¹ Au₃ ions. ◇: distributions at the termination of the full MD simulation (3 ps); and +: distributions following an additional 100 ps evolution period for the ejected material.

starting conditions. The same two-body potentials that were used in the sputtering program were used for the evolution program. The positions

and velocities of the sputtered atoms were saved to files at the end of the 100 ps evolution period. These files then were scanned for clusters

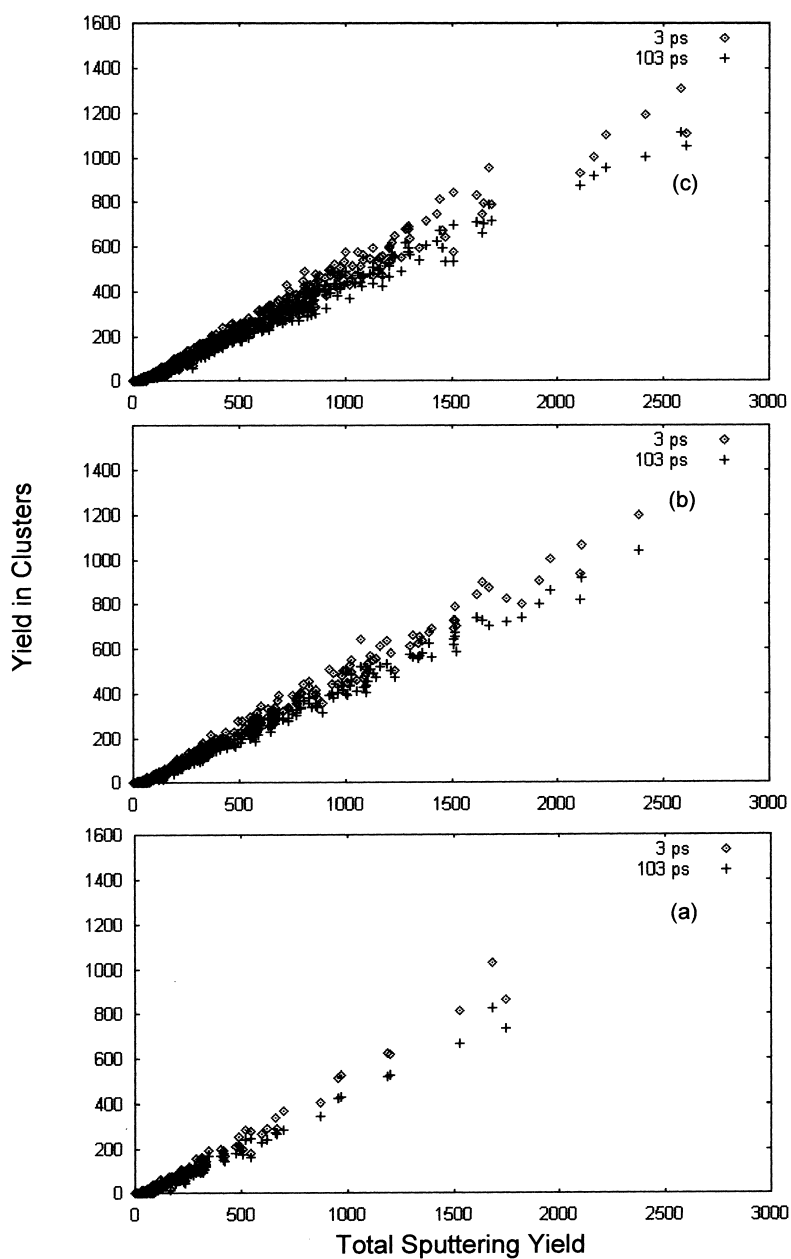


Fig. 2. Yields in clusters versus total yields for individual sputtering events following bombardment of Au(111) targets with (a) 100 keV Au₁ ions, (b) 100 keV atom⁻¹ Au₂ ions, and (c) 100 keV atom⁻¹ Au₃ ions. ◇: distributions at the termination of the full MD simulation (3 ps); and +: distributions following an additional 100 ps evolution period for the ejected material.

using the same criteria as before. This procedure ensured that all clusters that remained after unimolecular decomposition as well as clusters

formed by fragmentation, and any possible recombination mechanisms in the gas phase would be counted.

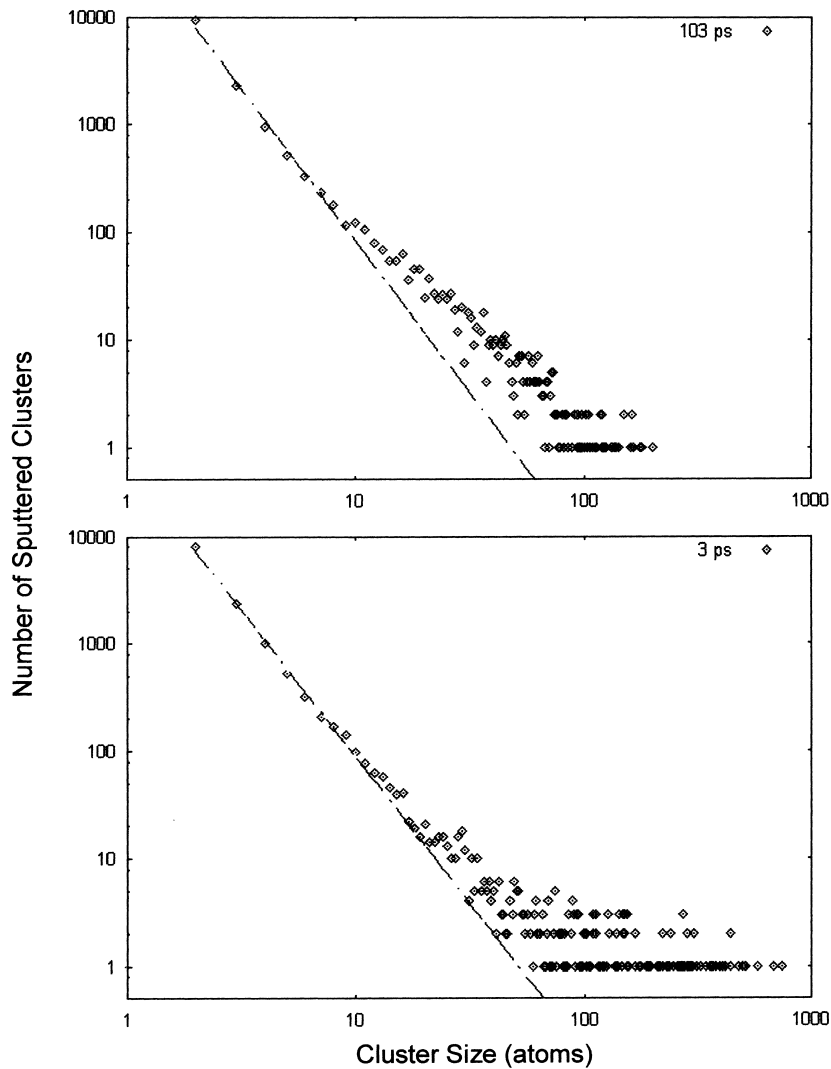


Fig. 3. Power-law fits to the size distributions of emitted clusters following the bombardment of Au(111) targets with $100 \text{ keV atom}^{-1} \text{ Au}_3$ ions at the termination of the full MD simulation (lower panel), and after an additional 100 ps evolution period for the ejected material (upper panel). Note that the power-law fits were done for $n < 9$ only.

Computer animations¹ of the evolution process were made for a few events that had relatively large total yields and relatively large clusters emitted initially from the target. These produced some interesting results that are described in detail below.

¹The computer animations are available online at <http://chaos.fullerton.edu/cluster-animations.html>

3. Results

Fig. 1a–c compare the yields of clusters with $n \geq 2$ before and after the 100 ps evolution period for Au_1 , Au_2 , and Au_3 impacts at $100 \text{ keV atom}^{-1}$ on nine-layer Au(111) targets. For all three cases the cluster yield distributions are similar both before and after the 100 ps evolution. For small clusters, $n \leq \sim 10$, the yields follow power-

law decreases. For $n \geq \sim 10$ the distributions deviate substantially from the power-law decreases, with many more large clusters being emitted than would be expected from the power-law. For each of the three cases, the largest clusters emitted at the termination of the basic sputtering simulation (3 ps) have > 700 atoms each.

While these very large clusters are not stable, clusters with ~ 200 or more atoms are seen after the 100 ps evolution period. Comparison of the cluster size distributions before and after evolution shows statistically significant *increases* in the number of clusters in the 10–100 atom range. This suggests that fragmentation as well as unimolecular decomposition takes place during the evolution process. Our computer animations, which owing to computer resource limitations included only a small fraction of the simulated events, support this notion. In the first 10 or so picoseconds the largest

clusters were seen to fragment into typically four or five smaller clusters. These smaller fragments often would *grow* in size through collisions with other clusters and individual atoms early in the evolution process. However, after the first 10–15 ps the larger clusters would lose atoms primarily through unimolecular decomposition. Much less frequently a very small cluster (dimer or trimer) would be shaken off one of the larger clusters.

Fig. 2a–c show the correlation between the total sputtering yield and the contribution to the yield from clusters. For those impacts with total yields $> \sim 100$, the correlation is very strong. At the end of the basic MD simulation (3 ps) roughly half of the yield is in the form of clusters with $n \geq 2$ provided that the total yield for the event exceeds ~ 100 atoms. The fraction of the yield in clusters drops to roughly 40% after the 100 ps evolution period.

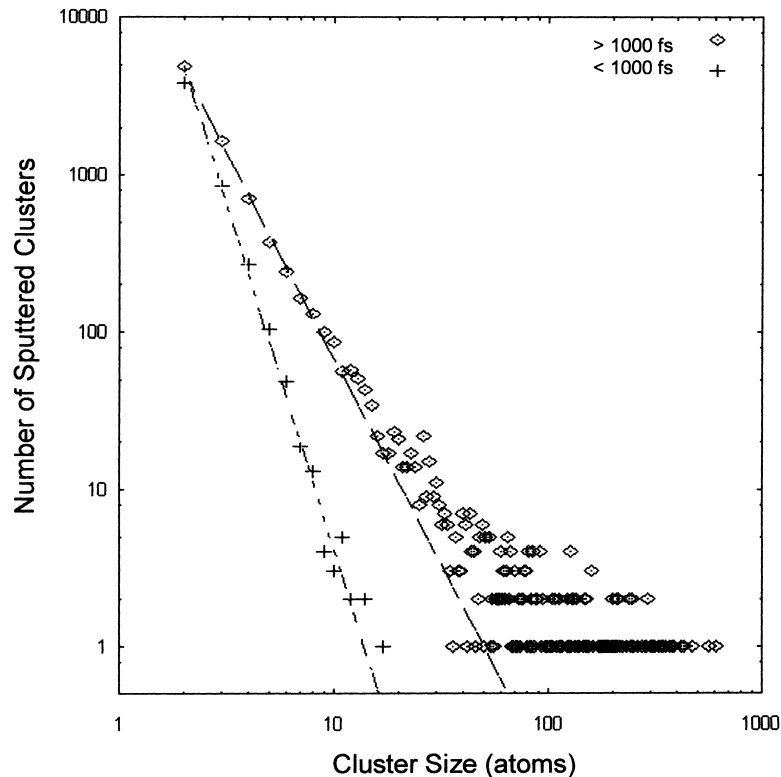


Fig. 4. Size distributions of clusters emitted during the ballistic phase (< 1000 fs), and clusters emitted during the thermal spike phase of the collision cascade (> 1000 fs) following bombardment of Au (111) targets with $100 \text{ keV atom}^{-1} \text{ Au}_3$ ions. Power-law fits for $n < 9$ also are shown.

Fig. 3a and b provide a more detailed view of the cluster size distributions for the $\text{Au}_3 \rightarrow \text{Au}(111)$ case at the end of the basic MD simulation (3 ps) and after an additional 100 ps evolution time. At 3 ps clusters with $n < \sim 30$ atoms follow a power-law with $Y \propto n^{-2.7}$. The major deviation from the power-law decrease in this case is for the clusters with $n > \sim 30$ atoms. After the 100 ps evolution, clusters with $n \leq 9$ atoms follow a power-law decrease with $Y \propto n^{-2.8}$. The deviation from the power-law decrease begins at $n = 10$ in this case, and the excess in the range from $n = 10$ to $n = 100$ clearly is larger than at 3 ps.

Since our earlier simulations [2] showed substantial contributions to the sputtering yield from the thermal spike phase of the collision cascade, we examined the dependence of cluster yield on emission time. While there is no sharp dividing line between the ballistic phase and the thermal spike phase, our previous results indicated that the ballistic phase was essentially complete by 1 ps. We examined separately clusters emitted before and after 1 ps in the simulations. The results for the $\text{Au}_3 \rightarrow \text{Au}(111)$ case are shown in Fig. 4. The $\text{Au}_1 \rightarrow \text{Au}(111)$ and $\text{Au}_2 \rightarrow \text{Au}(111)$ cases produced very similar results.

There is a striking difference between the distributions of clusters emitted before and after 1 ps. All the clusters emitted during the ballistic phase (before 1 ps) are relatively small ($n < \sim 20$), and their distribution follows a power-law decrease ($Y \propto n^{-4.4}$) quite closely. The distribution of clusters emitted during the thermal spike phase is quite different. Only the smallest clusters in this distribution ($n < \sim 10$) follow a power-law decrease (in this case $Y \propto n^{-2.6}$), and all of the very large clusters are emitted during the thermal spike phase.

4. Discussion

At bombarding energies up to several keV the yield versus size curve for emitted clusters generally follows a power-law decrease. While this behavior is not completely understood, recent studies [12,13] suggest that such behavior should be expected from the statistical model of cluster formation in ballistic sputtering. Our results for clusters emitted

during the ballistic phase for events initiated by projectiles with $100 \text{ keV atom}^{-1}$ are consistent with this model. However, another mechanism must be responsible for the emission of large clusters during the thermal spike phase of the collision cascade. Our results show that relatively large clusters of atoms can be lifted intact from the surface in the vicinity of the spike. The largest of these clusters quickly fragment into several intermediate size clusters. Some of the intermediate size clusters grow through collisions with other fragments, but eventually most clusters lose some of their constituent atoms through unimolecular decomposition before becoming relatively stable.

The small number of large-yield events that were examined with computer animations showed a strong tendency for the larger clusters to be ejected from periphery of the collision cascade. This suggests that the very large clusters that are emitted during the thermal spike phase come from the cooler regions at the edge of the spike. However, many more events would have to be examined in detail to verify this suggestion.

Acknowledgements

This work was supported in part by the National Science Foundation (Grants DMR-9712538 at Cal State Fullerton and DMR-9730893 at Caltech). The authors gratefully acknowledge the assistance of Josh Soneson and Deanna Smith, who prepared the computer animations.

References

- [1] H.H. Andersen, A. Brunelle, S. Della-Negra, J. Depauw, D. Jacquet, Y. LeBeyec, J. Chaumont, H. Bernas, Phys. Rev. Lett. 80 (1998) 5433.
- [2] M.H. Shapiro, T.A. Tombrello, Nucl. Instrum. Meth. B 152 (1999) 221.
- [3] T.J. Colla, H.M. Urbassek, A. Wucher, C. Staudt, R. Heinrich, B.J. Garrison, C. Dandachi, G. Betz, Nucl. Instrum. Meth. B 143 (1998) 284.
- [4] K. Gärtner et al., Nucl. Instrum. Meth. B 102 (1995) 183.
- [5] M.H. Shapiro, T.A. Tombrello, D.E. Harrison Jr., Nucl. Instrum. Meth. B 30 (1988) 152.

- [6] J. Lindhard, M. Scharff, H.E. Schiott, K. Dan. Vidensk. Selsk. Mat. Fys. Medd. 33 (1963) 14.
- [7] D.A. Bromley, in: S.P. Parker (Ed.), McGraw-Hill Encyclopedia of Physics, second edn, McGraw-Hill, New York, 1993, p. 276.
- [8] M.H. Shapiro, T.A. Tombrello, Nucl. Instrum. Meth. B 58 (1991) 161.
- [9] M.H. Shapiro, Rad. Effects Defects Sol. 142 (1997) 259.
- [10] M.H. Shapiro, T.A. Tombrello, Nucl. Instrum. Meth. B 84 (1994) 453.
- [11] A. Wucher, B.J. Garrison, Phys. Rev. B 46 (1992) 4855.
- [12] J.W. Hartman, M.H. Shapiro, T.A. Tombrello, Nucl. Instrum. Meth. B 124 (1997) 31.
- [13] J.W. Hartman, M.H. Shapiro, T.A. Tombrello, Nucl. Instrum. Meth. B 132 (1997) 406.